J. Phys. B: At. Mol. Opt. Phys. **45** (2012) 115302 (8pp) doi:10.1088/0953-4075/45/11/115302

Three-dimensional solitons in cross-combined linear and nonlinear optical lattices

F Kh Abdullaev[1], A Gammal[2], H L F da Luz[2], M Salerno[3] and Lauro Tomio[4,5]

[1] CFTC, Complexo Interdisciplinar, Universidade de Lisboa, 1649-003, Portugal
[2] Instituto de Física, Universidade de São Paulo, 05508-090, São Paulo, SP, Brazil
[3] Dipartimento di Fisica ER Caianiello, CNISM and INFN - Gruppo Collegato di Salerno, Università di Salerno, Via Ponte don Melillo, 84084 Fisciano (SA), Italy
[4] Instituto de Física, Universidade Federal Fluminense, 24210-346, Niterói, RJ, Brazil
[5] Instituto de Física Teórica, Universidade Estadual Paulista (UNESP), 01140-070, São Paulo, SP, Brazil

E-mail: tomio@ift.unesp.br

Received 9 February 2012, in final form 9 April 2012
Published 18 May 2012
Online at stacks.iop.org/JPhysB/45/115302

Abstract
The existence and stability of three-dimensional (3D) solitons, in cross-combined linear and nonlinear optical lattices, are investigated. In particular, with a starting optical lattice (OL) configuration such that it is linear in the x-direction and nonlinear in the y-direction, we consider the z-direction either unconstrained (quasi-2D OL case) or with another linear OL (full 3D case). We perform this study both analytically and numerically: analytically by a variational approach based on a Gaussian ansatz for the soliton wavefunction and numerically by relaxation methods and direct integrations of the corresponding Gross–Pitaevskii equation. We conclude that, while 3D solitons in the quasi-2D OL case are always unstable, the addition of another linear OL in the z-direction allows us to stabilize 3D solitons both for attractive and repulsive mean interactions. From our results, we suggest the possible use of spatial modulations of the nonlinearity in one of the directions as a tool for the management of stable 3D solitons.

1. Introduction

The investigation of solitons in media with periodically modulated parameters is a recent topic attracting a great deal of interest, in view of the possibilities of achieving nonlinear wave management in concrete applications. In particular, the existence of stable gap solitons has been theoretically demonstrated and experimentally confirmed in periodic nonlinear systems such as Bose–Einstein condensates (BEC) in optical lattices and nonlinear optical fibres with periodic modulations of the refraction index [1–3].

The treatment of stable multidimensional solitons in nonlinear media, with periodic linear parameters, has been done in [4]. In particular, two-dimensional (2D) solitons have been investigated in [5–7], while the existence of three-dimensional (3D) gap solitons has been reported in [8, 9]. In [8], it has been shown that, while finite energy solitary waves in shallow nonlinear periodic structures can be stable in the whole band gap region in the 2D case, they can be stabilized only in certain regions of the band gap in the 3D case.

The authors of [9] also considered the existence and stability of families of 3D solitons in self-focusing cubic Kerr-type optical media with an imprinted 2D harmonic transverse modulation of the refractive index. Moreover, the existence of 3D optical solitons, also called light bullets, in a 2D spatial lattice with one temporal dimension, has been shown in [10, 11]. Examples of these are: light bullets in radial tandem structures [10] and in Bessel OLs with out-of-phase modulation of a linear optical lattice (LOL) [11]. In [12], a study considering collisions between solitons in the 3D self-attractive BEC loaded into deep 2D OLs was reported. More recently, in [13], the generation of stable 3D solitary waves spatio-temporally localized in waveguide arrays (discrete light bullets) has been demonstrated.

Both in nonlinear optics and in the context of BEC, the nonlinear parameters can be modulated in space and/or in time quite easily [14, 15]. In optics, one usually deals with materials having quadratic or cubic nonlinear susceptibilities, e.g. $\chi^{(2)}$ and $\chi^{(3)}$. The variation of the nonlinearities can be achieved by considering different approaches, including layered structures with different values of the Kerr nonlinearity, photonic crystals with the holes infiltrated by highly nonlinear liquids, waveguide arrays with titanium doped $LiNbO_3$ crystals, arrays in glass written by a high intensity femtosecond laser [16]. In BEC, the mean field nonlinearity coefficient is proportional to the atomic scattering length [17] and can be tuned in space by using the Feshbach resonance technique, considering either the magnetic external field periodically varying in space [18] or by using optically induced Feshbach resonances by standing laser fields [19, 20].

In all of these contexts, periodic structures involving modulations of the nonlinearity or combined modulations of the linear and nonlinear parameters are possible [11, 21, 22]. In the following, we refer to *nonlinear optical lattices* (NOL) as the cases where a lattice results from a pure periodic modulation of the nonlinear parameter. This type of lattice, recently realized in experiments [23], has been discussed in several numerical and theoretical works, leading to interesting new effects in the 1D case. In this respect we mention: stable solitons in 1D optical lattice [24], matter-wave optical limiting process and bistability [25], long-lived Bloch oscillations [26] and dynamical localization [27] of gap solitons, linear superpositions of matter waves [28], stable localized states in random NOL [29], filter solitons [30], etc.

Theoretical and numerical investigations of 2D solitons in the presence of 1D NOL have also been performed. In particular, it has been shown that narrow solitons located at the maxima of nonlinear smooth periodic modulations can exist, but they have a region of stability so small that they can be considered unstable for any practical purpose [31]. Sharp 1D NOL in the form of 1D stripes with box-shaped profiles have been shown to support stable 2D solitons [32] in a narrow window of number of atoms.

On the other hand, for smooth cross-combined 2D OLs (e.g., 1D LOL in one direction and 1D NOL in the other), it has been recently demonstrated that stable 2D solitons can exist for a wide range of parameters [33]. The dynamics and stability of solitons in 2D BEC were also investigated in [34] for dissipative nonlinear optical lattices with a conservative interaction in one of the spatial directions.

For binary mixtures in BEC, considering NOL, the soliton stability has been explored in [35] for the 1D case, and more recently in [36] for the 2D case. In the presence of inhomogeneities and dissipative perturbations, the stability and dynamics of matter-wave vortices are investigated in [37]. In contrast to the above 1D and 2D studies, the occurrence of 3D solitons in continuous periodic structures, with spatial variations of the nonlinearity, has been scarcely investigated.

The aim of this paper is to investigate, both analytically and numerically, the existence and stability of matter-wave 3D solitons in crossed-combined OL systems consisting of a smooth NOL in one direction, defined as the y-direction, with one or two LOLs in the remaining two perpendicular directions, defined as the x- and z-directions. More precisely, by fixing that in the x-direction we have a LOL, the z-direction is taken either as unconstrained (quasi-2D cross-combined OL) or with another LOL (full 3D cross-combined OL). In the former case, we study only the case of attractive mean nonlinearities due to the fact that for repulsive mean interactions localization is obviously impossible in the unconstrained direction. In the latter case, both attractive and repulsive mean nonlinearities are considered.

As a main result we show that while in the quasi-2D cross-combined OLs (e.g. with a LOL and a NOL) 3D solitons are always unstable, the addition of another linear OL in the remaining orthogonal direction (z-direction) allows us to stabilize 3D solitons not only for attractive but also for repulsive interatomic mean interactions, a result which can be of interest for practical applications. In this respect we remark that while attractive 3D solitons are subjected to strong collapses and to delocalizing transitions [38], no collapse exists for repulsive interactions. The existence and stability of 3D regions for solitons in parameter space can be much wider, being limited only by delocalizing thresholds [38].

Our analytical considerations are based on a Gaussian variational approach (VA), for the condensate wavefunction with different parameters for the three directions, to account for elliptical cross sections of the 3D solitons induced by the lattice anisotropy. The results of the VA analysis are presented in terms of the chemical potential and number of atoms dependence, and compared with numerical results obtained by relaxation methods [39] and by direct numerical integrations of the Gross–Pitaevskii (GP) partial differential equation (PDE). The stability properties of the 3D solitons are investigated both by direct GPE time evolutions of the soliton profiles and by VA, using the Vakhitov–Kolokolov (VK) criterion [40] for a necessary condition for soliton stability[6].

In our analysis, the cross-combined LOLs and NOL are always arranged to have a minimum in the origin for all corresponding spatial directions so that a Gaussian centred at the origin can be a good ansatz for 3D solitons. Configurations of the OLs in which a minimum of one type of OL corresponds to a maximum of another are obviously possible, but they induce distortions of the wavefunction in different directions making a Gaussian VA inappropriate and leading to instabilities. From numerical investigations of such 'distorted' waves, indeed, we have always found that they are unstable and as such we have discarded them from this paper.

We finally remark that, in analogy with what has been done for the 1D case, the stabilization of 3D solitons in the presence of a NOL in one of the spatial directions introduces the possibility of using the modulation of the scattering length as a tool for 3D soliton management. We should note that multidimensional solitons have not yet been created in real experiments with BEC. Therefore, cross-combined linear and nonlinear OLs could provide another alternate approach to fulfil this task.

The paper is organized as follows. In section 2, we introduce the model formalism and discuss the physical implementation of 2D crossed linear and nonlinear lattices

[6] See also a discussion on this criterion in [41, 42].

using spatial modulations of the scattering length. In section 3, we derive the VA equations for 3D BEC solitons with attractive mean interaction in a quasi-2D cross-combined OL, with the unconstrained z-direction. The results of this analysis are also compared with direct calculations of the GP PDE. In section 4, we consider 3D BEC solitons trapped in a cross-combined 2D LOL and 1D NOL in the case of both attractive or repulsive mean interatomic interactions. The VA equations, derived for equal signs of the OLs strengths, are compared with direct integrations of the GP equation. The parameter regions with stable solitons are also verified by considering both the VK criterion and direct time propagation of the GP solutions. Finally, in section 5, we conclude with a summary of the main results of this work.

2. Model equations and analysis

We take as a model for 3D BEC in cross-combined OLs in the mean field approximation the following GP equation:

$$\mathrm{i}\hbar\frac{\partial\psi}{\partial t} = -\frac{\hbar^2}{2m}\nabla^2\psi - \sum_{\zeta=x,z}\Lambda_\zeta\cos(2k\zeta)\psi + g(y)|\psi|^2\psi, \quad (1)$$

where $\psi \equiv \psi(\mathbf{r},t)$ is normalized to the number of atoms, ∇^2 denotes the 3D Laplacian, m is the atomic mass and $\Lambda_\zeta\cos(2k\zeta)$ is a LOL in the ζ-directions ($\zeta \equiv x,z$), with strength Λ_ζ and lattice constant π/k (assumed to be identical in both directions ζ). The $g(y)$ represents a NOL in the y-direction with the following form:

$$g(y) = g_0 + g_1\cos(2\kappa y), \quad (2)$$

where g_0 denotes the mean nonlinearity related to the mean s-wave scattering length a_{s0}, given by $g_0 = 4\pi\hbar^2 a_{s0}/m$ for 3D, and g_1 is the strength of a periodic modulation of the nonlinearity in the y-direction having the period π/κ.

The spatial modulation of the nonlinear parameter (interaction) can be produced either by spatially varying magnetic fields near a Feshbach resonance or by optically induced Feshbach resonances [19]. In the last case, the scattering length is manipulated with a laser field tuned near a photo association transition, e.g., close to the resonance of one of the bound p levels of the excited molecules. Virtual radiative transitions of a pair of interacting atoms to this level can change the value and even reverse the sign of the scattering length. It can be shown [19] that a periodic variation of the laser field intensity in the y-direction, such as $I(y) = I_0\cos^2(\kappa y)$, produces a periodic variation of the atomic scattering length of the form $a_s(y) = a_{s0}[1+\alpha I/(\delta+I)]$, where a_{s0} is the scattering length in the absence of light, δ is the frequency detuning of the light from the resonance and α is a constant factor [19, 24]. For weak intensities, e.g., when $I_0 \ll |\delta|$, we have that the real part of the scattering length can be approximated by $a_s = a_{s0}+a_{s1}\cos^2(\kappa y)$, leading to a modulated nonlinearity of essentially the same form as assumed in equation (2).

It is worthwhile to note that the creation of a NOL in a BEC also implies some spontaneous emission loss which is inherent in the optical Feshbach resonance technique. Here we assume that such dissipative effects can be ignored, this being possible if one uses laser fields detuned from the resonance and of intensity sufficiently high [43]. (Similar conclusions would also be reached for periodic variation of the scattering length induced by the usual Feshbach resonance technique.)

In the following, we adopt dimensionless units by scaling space and time variables such that the variables in (1) are replaced according to $t \to (\hbar/E_r)\,t$, $\mathbf{r} \to \mathbf{r}/k$, with $E_r \equiv \hbar^2k^2/2m$ being the recoil energy and $\mathbf{r} \equiv x,y,z$. The wavefunction is rescaled as $\psi(\mathbf{r},t) \to k^{3/2}u(\mathbf{r},t)$, in terms of which equation (1) acquires the form

$$\mathrm{i}\frac{\partial u}{\partial t} = -\nabla^2 u - Vu - \Gamma|u|^2u, \quad (3)$$

where

$$V \equiv V(x,z) = \varepsilon_x\cos(2x) + \varepsilon_z\cos(2z) \quad (4)$$

$$\Gamma \equiv \Gamma(y) = \chi + \gamma\cos(\lambda y) \quad (5)$$

denote the linear and nonlinear OLs, respectively. Considering equations (1)–(3), we have the following definitions:

$$\varepsilon_\zeta \equiv \Lambda_\zeta/E_r, \quad \chi \equiv g_0k^3/E_r = -8\pi a_{s0}k,$$
$$\lambda \equiv 2\kappa/k, \quad \gamma \equiv -g_1k^3/E_r, \quad (6)$$

with g_1 being assumed as a free parameter.

For the stationary solutions corresponding to equation (3), we redefine the above wavefunctions $u(\mathbf{r},t)$ as $u(\mathbf{r},t) = U(x,y,z)\,\mathrm{e}^{\mathrm{i}\mu t}$, where μ is the chemical potential. Therefore, the stationary equation for U is given by

$$\mu U + \nabla^2 U + VU + \Gamma|U|^2U = 0, \quad (7)$$

from which the chemical potential and corresponding total energy are, respectively, given by

$$\mu N = \int\{|\nabla U|^2 - V(x,z)U^2 - \Gamma(y)U^4\}\,\mathrm{d}x\,\mathrm{d}y\,\mathrm{d}z, \quad (8)$$

$$E = \frac{1}{2}\int\left\{|\nabla U|^2 - V(x,z)U^2 - \frac{\Gamma(y)}{2}U^4\right\}\mathrm{d}x\,\mathrm{d}y\,\mathrm{d}z. \quad (9)$$

The integrations in the above and following expressions cover the 3D phase space from $-\infty$ to $+\infty$.

2.1. Variational analysis

In order to develop a variational analysis of equations (7)–(9), we consider the following ansatz:

$$U(x,y,z) = A\,\mathrm{e}^{-\frac{1}{2}(ax^2+by^2+cz^2)}, \quad (10)$$

where a, b and c are the parameters controlling the widths of the Gaussian in the three directions. We remark that this ansatz assumes that the BEC density remains centred at the origin and therefore is appropriate when the signs of the LOL ε and of NOL γ are equal (both positive). For opposite signs, say $\varepsilon > 0$ and $\gamma < 0$, indeed, an origin-centred Gaussian ansatz is clearly not good due to the different positions of the minima of LOL and NOL in the x- and y-directions, respectively. This fact is easily understood if one thinks that, while in the x-direction the matter tends to localize around the origin at $x = 0$ (due to a minimum of the LOL there), in the y-direction the NOL has a maximum at $y = 0$ (the local interaction is repulsive) and the matter tends to delocalize there. This leads to a distortion of

the density in the xy-plane, which cannot be described by the simple ansatz (10). From PDE simulations (as we mentioned before), we found that such distorted solutions can exist, but they are always unstable. Therefore, in the following we shall restrict the VA to the case of $\varepsilon > 0$ and $\gamma < 0$, for which the ansatz (10) is appropriate.

From (10), the normalized number of atoms is expressed in terms of the variational parameters A, a, b and c:

$$N = \int U^2 \,\mathrm{d}x\,\mathrm{d}y\,\mathrm{d}z = \frac{A^2\pi^{3/2}}{\sqrt{abc}}. \tag{11}$$

The stationary GP equation in (7) can be derived from the field Lagrangian L, which is given by

$$2L = \int \left\{ |\nabla U|^2 - [\mu + V(x,z)]U^2 - \frac{\Gamma(y)}{2}U^4 \right\} \mathrm{d}x\,\mathrm{d}y\,\mathrm{d}z. \tag{12}$$

By substituting the ansatz (10) into the above Lagrangian and performing the integrations, in terms of the variational parameters a, b, c and A, we obtain the following effective Lagrangian:

$$L_{\mathrm{eff}} = \frac{A^2\pi^{\frac{3}{2}}}{4\sqrt{abc}}\left\{ a+b+c - \frac{A^2}{2\sqrt{2}}\left[\chi + \gamma\,\mathrm{e}^{-\frac{\lambda^2}{8b}}\right] - 2(\mu + \varepsilon_x\,\mathrm{e}^{-\frac{1}{a}} + \varepsilon_z\,\mathrm{e}^{-\frac{1}{c}}) \right\}, \tag{13}$$

with A^2 being linked to the number of atoms by relation (11).

The above formalism with the corresponding variational treatment refers to a more general study on the stability of systems with crossed-combined linear and nonlinear optical lattices. With respect to parameters, ε_x and ε_z, of the LOLs, in the next two sections we consider two specific cases: (i) $\varepsilon_x \equiv \varepsilon$ with $\varepsilon_z = 0$, implying a cross-combined 1D LOL with 1D NOL; and (ii) $\varepsilon_x \equiv \varepsilon_z \equiv \varepsilon$, implying a cross-combined 2D LOL with 1D NOL.

3. 3D solitons in cross-combined quasi-2D OLs

In this section we discuss the possibilities of the existence of 3D solitons in cross-combined quasi-2D OLs, with no constraints in the z-direction, e.g., we consider $\Lambda_z = 0$ in equation (1), corresponding to $\varepsilon_z = 0$ in equation (4). Our attention will be concentrated only on the case of attractive mean interactions, the only possibility one may think for the existence of 3D solitons with one of the directions unconstrained.

By considering $\varepsilon_z = 0$ and $\varepsilon_x \equiv \varepsilon$ in equation (13), an implicit relation between the chemical potential and the number of atoms can be obtained from the corresponding Euler–Lagrange equations for the parameters a, b, c and A. Therefore, in terms of these variational parameters, we have the following expressions for the chemical potential μ and for the number of particles N, respectively:

$$\mu = \frac{b}{2} - a - \varepsilon\left(1 - \frac{3}{a}\right)\mathrm{e}^{-\frac{1}{a}}, \tag{14}$$

$$N = 4\pi\sqrt{\frac{2\pi}{abc}}\,\frac{a - 2\varepsilon\left(\mathrm{e}^{-\frac{1}{a}}\right)/a}{\chi + \gamma\,\mathrm{e}^{-\frac{\lambda^2}{8b}}}, \tag{15}$$

where a, b and c satisfy the following transcendental equation:

$$\frac{1}{b} + \frac{\lambda^2}{4b^2}\,\frac{\gamma\,\mathrm{e}^{-\frac{\lambda^2}{8b}}}{\chi + \gamma\,\mathrm{e}^{-\frac{\lambda^2}{8b}}} = \frac{1}{c}, \tag{16}$$

with the parameter c being given by

$$c = \left(a - \frac{2\varepsilon}{a}\,\mathrm{e}^{-1/a}\right). \tag{17}$$

With the above, we can rewrite expression (15) for the number of particles as

$$N = 4\pi\sqrt{\frac{2\pi c}{ab}}\,\frac{1}{\chi + \gamma\,\mathrm{e}^{-\frac{\lambda^2}{8b}}}. \tag{18}$$

Obtained from the above equations, for different strengths of the LOL in the x-direction (as shown inside the figure), with the z-direction being unconstrained ($\varepsilon_z = 0$), in the top panel of figure 1 we depict the resulting curves of 3D solitons in the $\mu - N$ plane. As verified, no stable 3D solitons are predicted to exist, according to the VK criterion, which predicts stability for $\mathrm{d}\mu/\mathrm{d}N < 0$ in the attractive case.

In the bottom panel of figure 1, we have compared one of the VA curves (for $\varepsilon_x = 3$) with the corresponding one being obtained from numerical simulations of the GP equation, from where we observe a good quantitative agreement between numerical and analytical results. The PDE simulations also confirm the prediction of the VK criterion about the instability of 3D solitons in this case.

In the next section, we consider the second case treated in this work, with LOL in both x- and z-directions.

4. Solitons in cross-combined full 3D OLs

The result of the previous section obviously cannot be valid for repulsive scattering lengths, with the z-direction being fully unconstrained. However, for the repulsive case, we can stabilize solitons by adding a linear OL in the z-direction. Therefore, in this section we will follow the previous derived equations, leading to the variational effective Lagrangian (13), considering the specific symmetric LOL case, with $\varepsilon_x = \varepsilon_z \equiv \varepsilon$. With such assumptions, for symmetry reasons, the stationary soliton solutions will have equal widths in the x-and z-directions, with the ansatz U having $c = a$. At the end of this section, in our dynamical numerical simulations, we also reduce the LOL strength in the z-direction in order to have a more clear picture on the transition from a stable to an unstable regime.

Following the same discussion in the previous section on the validity of the Gaussian ansatz for 3D solitons in cross-combined OLs, we also restrict here the signs of the two LOLs and of the NOL to be the same (all positive). The effective Lagrangian in this case is given by

$$L_{\mathrm{eff}} = \frac{\pi^{3/2}A^2}{4a\sqrt{b}}\left\{ 2a + b - 2(\mu + 2\varepsilon\,\mathrm{e}^{-1/a}) - \frac{A^2}{2\sqrt{2}}(\chi + \gamma\,\mathrm{e}^{-\lambda^2/8b}) \right\}, \tag{19}$$

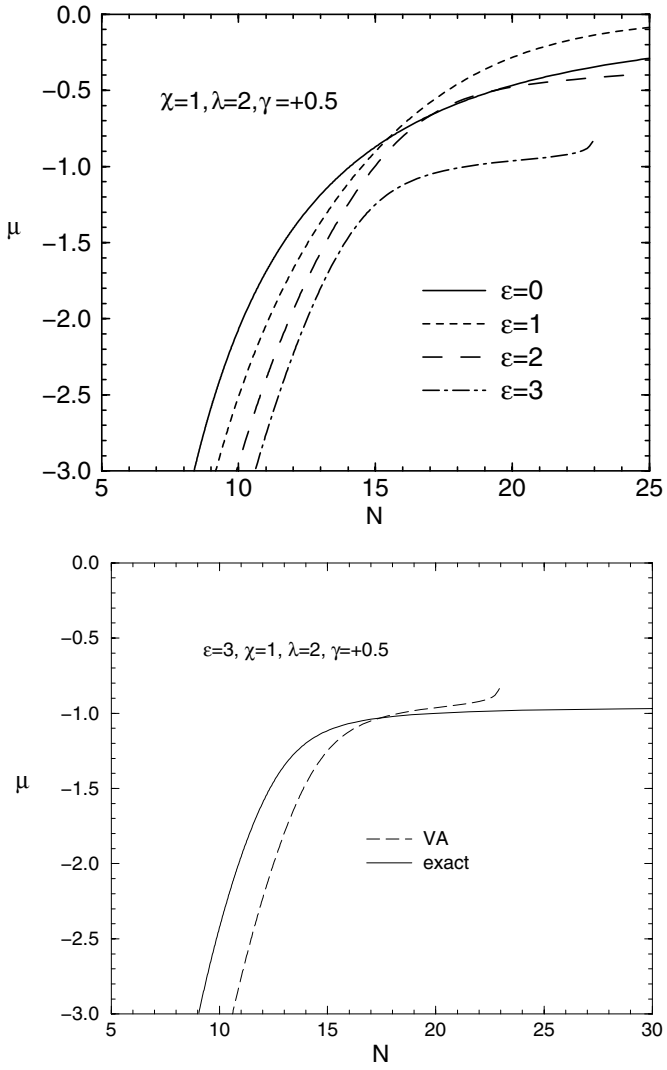

Figure 1. The chemical potential μ is presented in terms of the number of atoms N for 3D solitons in both panels, for crossed 1D LOL (x-direction) with 1D NLOL (y-direction), without any constraint in the third z-direction ($\varepsilon_z = 0$), considering attractive mean two-body interactions ($\chi = 1$). In the upper panel, we show the VA results for several strengths of the LOL $\varepsilon_x = \varepsilon$, with other parameters remaining fixed as given inside the frame. In the lower panel, we present a comparison between the VA results for $\varepsilon = 3$ (dashed line) with PDE results (solid line).

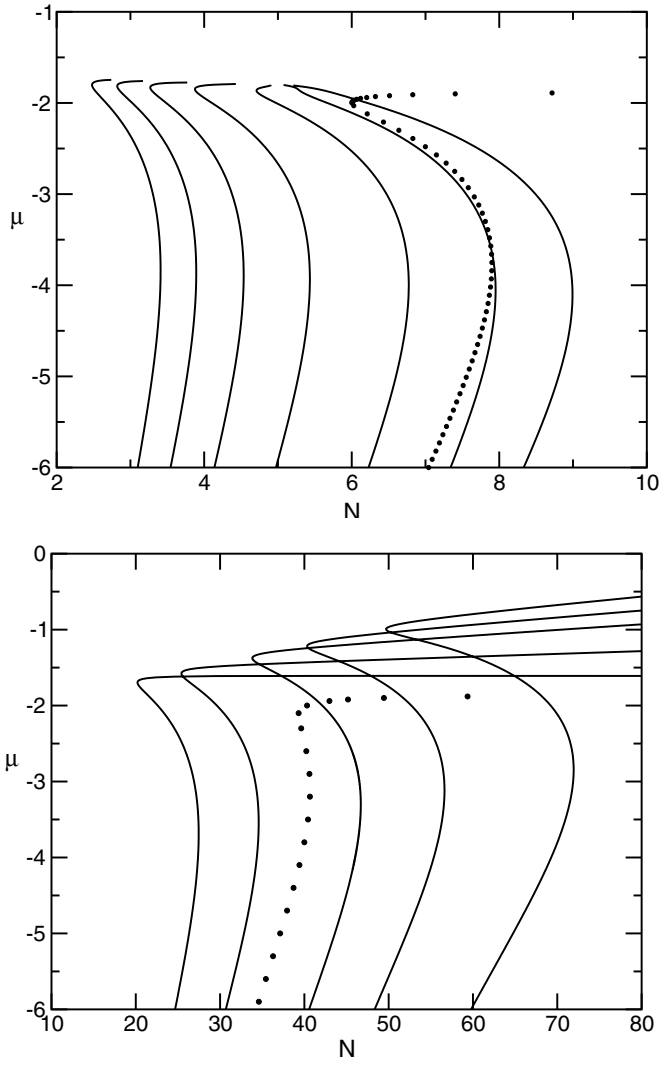

Figure 2. The chemical potential μ is presented in terms of the number of atoms N, considering VA results (solid lines) for 3D solitons in cross-combined 2D LOL and 1D NOL. In the upper panel, we fix ε =3 and the attractive interaction $\chi = 1$, varying the NOL strength, such that, from left to right, $\gamma = 3.0$, 2.5, 2.0, 1.5, 1.0, 0.7, 0.5, respectively. The PDE calculations are represented by the dotted curve for $\gamma = 0.5$ (other parameters are the same as in the case of VA). In the lower panel, with fixed parameters ε =3 and $\gamma = 0.5$, we consider several repulsive mean nonlinearity interactions. From left to right we have $\chi = 0.0$, -0.1, -0.2, -0.25, -0.3, respectively. In this case, the PDE calculations are represented by the dotted curve for $\chi = -0.2$ (keeping the same other parameters).

with A^2 being linked to the number of atoms by the relation

$$N = \frac{A^2 \pi^{3/2}}{a\sqrt{b}}.$$

In this case, we obtain the following relations for the chemical potential and the number of atoms in terms of the variational parameters:

$$\mu = \frac{b}{2} - a - 2\varepsilon \left(1 - \frac{2}{a}\right) \mathrm{e}^{-1/a}, \tag{20}$$

$$N = 4\pi \sqrt{\frac{2\pi}{b}} \frac{1 - 2\varepsilon(\mathrm{e}^{-1/a})/a^2}{\chi + \gamma\, \mathrm{e}^{-\lambda^2/8b}}. \tag{21}$$

As in equations (16) and (17), the parameters a and b are related by the following transcendental equation:

$$\frac{1}{b} + \frac{\lambda^2}{4b^2} \frac{\gamma\, \mathrm{e}^{-\frac{\lambda^2}{8b}}}{\chi + \gamma\, \mathrm{e}^{-\frac{\lambda^2}{8b}}} = \frac{1}{a - (2\varepsilon/a)\, \mathrm{e}^{-1/a}}. \tag{22}$$

In figure 2, we depict the resulting VA curves (continuous lines) in the plane ($\mu - N$) to consider the possible existence of stable 3D solitons in cross-combined 2D LOL and 1D NOL for both attractive and repulsive atomic interactions. As we observe, in both cases there are branches of the curves for which stable 3D solitons are predicted to exist by

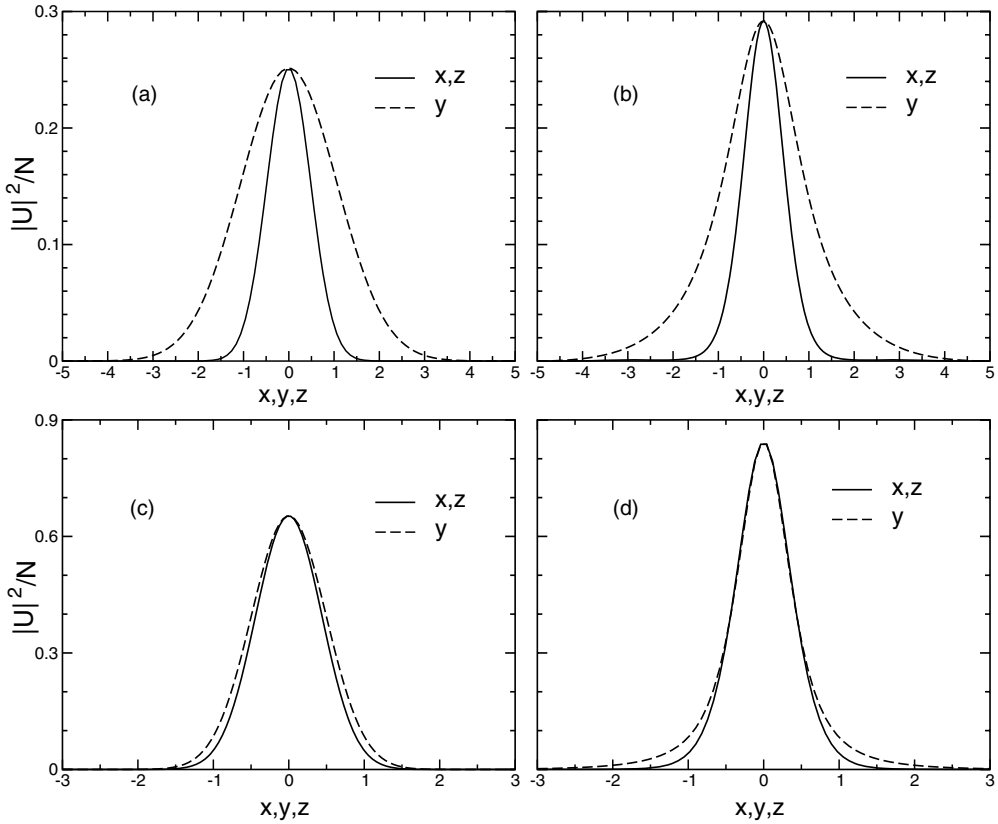

Figure 3. Upper panels: sections of the soliton profile as functions of one of the dimensions (with the other two fixed to zero) as obtained from the VA (panel (a)) and from PDE simulation (panel (b)), for attractive mean nonlinearity $\chi = 1$. For the NOL parameter we have $\gamma = 0.5$. The parameters of VA profiles are $a = c = 2.11$, $b = 0.44$, corresponding to $N = 6.5$ and $\mu = -2.07$. The values of N and μ for the PDE profiles are 5.84 and -2.07, respectively. Other parameters are fixed as in figure 2. Lower panels: the same as in the upper panels, but for a repulsive mean nonlinearity with $\chi = -0.2$. The parameters of the VA profiles (panel (c)) are $a = c = 2.589$, $b = 2.035$, corresponding to $\mu = -2.5$. The values of N and μ for the PDE profiles (panel (d)) are 40 and -2.5, respectively.

considering the VK criterion ($\mathrm{d}\mu/\mathrm{d}N < 0$). For comparison with the VA results (solid lines), we include in each panel of figure 2 the results obtained from direct PDE calculations showing numerically found stable solitons (dotted curves) for specific samples of parameters. We remark that although for repulsive interactions the VK criterion may not be indicative of gap soliton stability (sometimes, indeed, stability may be verified by an 'anti-VK criterion' $\mathrm{d}\mu/\mathrm{d}N > 0$ [42]), for the investigated cases we have always found a good agreement between VK predictions and numerical results.

Typical sections of soliton profiles, for 3D solitons obtained from VA, are depicted in the left panels of figure 3, for attractive (panel (a)) and repulsive (panel (c)) mean interactions. The corresponding soliton profiles, determined by the relaxation method, are shown in the right panels ((b) and (d)) of figure 3. We see that, while in the attractive case the agreement is quite good also from a quantitative point of view (see the upper panel of figure 2), for repulsive mean interactions the agreement becomes more qualitative, at least for the LOL and NOL parameters used. The observed discrepancy may be due to the inaccuracy of the Gaussian ansatz to describe the wavefunction of the condensate for larger values of the strength of the LOL. In the case of repulsive mean interactions and deep OLs, we have an unavoidable splitting of the condensate due to tunnelling of the matter into adjacent potential wells. In order to reduce the discrepancy and to improve the validity of the Gaussian ansatz, one should reduce the strength of the LOL as well as the strength of the mean nonlinearity.

In figure 4, we show the performed direct numerical time integrations of the GP equation for two specific points in the numerical curve given in figure 2. The two points, for $\mu = -2.5$ (top panel, stable solution) and $\mu = -3.5$ (bottom panel, unstable solution), are close to the limit that defines the stable/unstable region according to the VK criterion. The numerical simulations shown in figure 4 confirm that for $\mu = -2.5$ we have a stable solution, whereas the solution becomes unstable for $\mu = -3.5$. In the bottom panel of figure 4, one can see that immediately after the beginning of the dynamics the wavefunction exhibits strong oscillations, in contrast to the stable solution on the top panel, which remains the same for very long time. In figures 4 and 5 the soliton profiles in the different directions at each time have been overlapped for graphical convenience. The x- and z-direction profiles are identical, and the y-direction profile (affected by the NOL) is slightly wider (one can clearly see this near the ± 1.5 position). In this case, we have $\varepsilon = 3.0$, $\gamma = 0.5$ and repulsive mean nonlinearity $\chi = -0.2$.

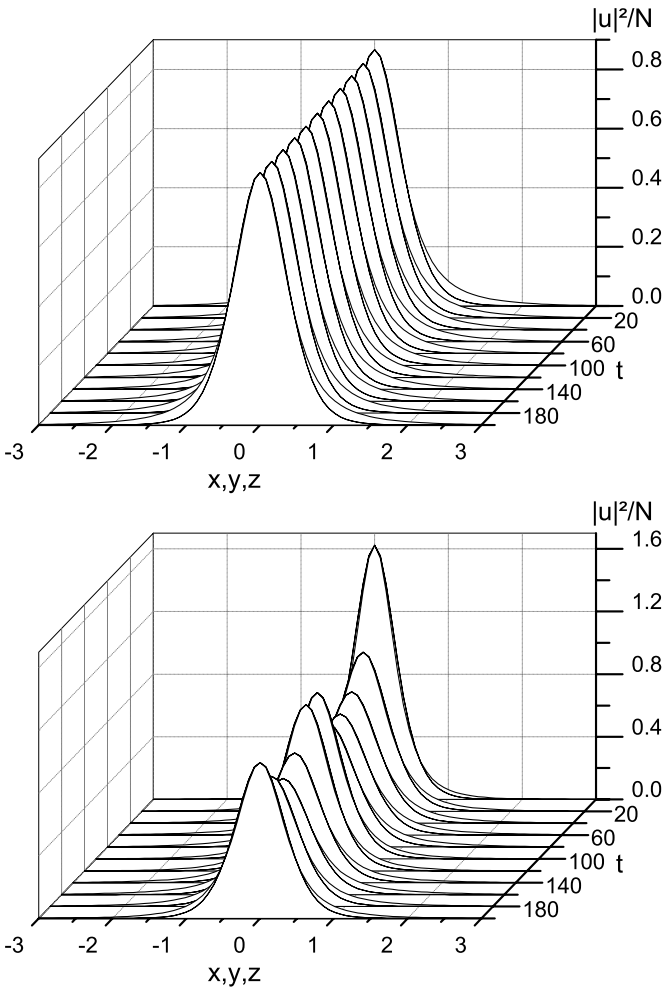

Figure 4. The dynamics of the solitons corresponding to two different regions of the lower panel of figure 2 (repulsive case). In the upper panel, with $\mu = -2.5$, we note the existence of a stable solution. In the lower panel, with $\mu = -3.5$, we observe that the solution becomes unstable. In both cases we have ε =3.0, $\gamma = 0.5$ and $\chi = -0.2$. The profile in the y-direction is slightly wider. Results are shown in dimensionless units.

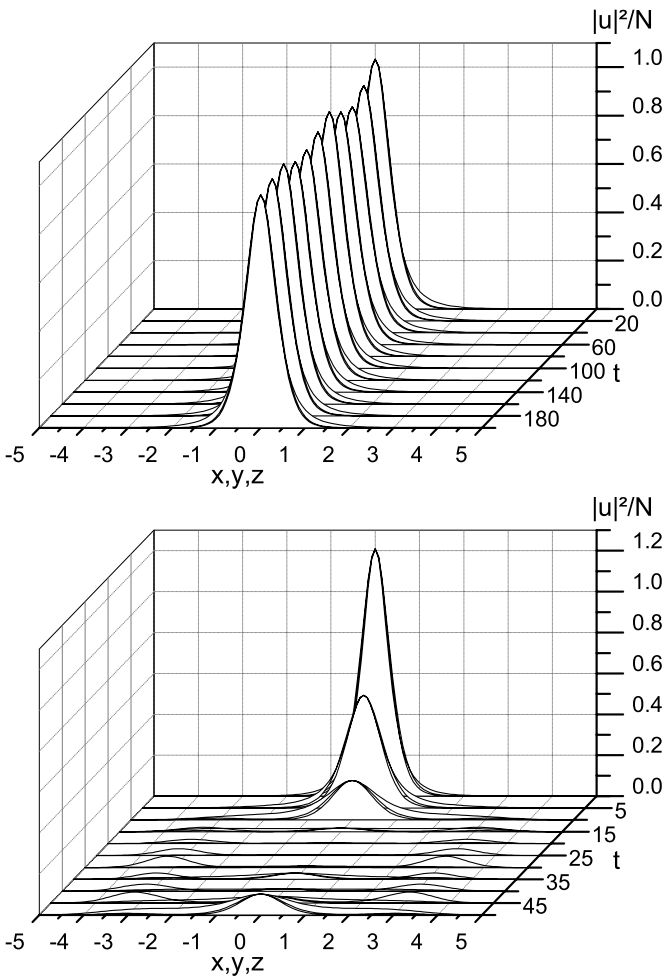

Figure 5. Loss of stability due to the reduction of the linear parameter in one direction, from $\varepsilon_z = 3.0$ (shown in the upper panel of figure 4) to $\varepsilon_z = 2.5$ (upper panel of this figure) and $\varepsilon_z = 2.0$ (lower panel of this figure). As shown in the lower panel, the instability occurs in a very short time interval. In both the cases we have $\varepsilon_x = 3.0$, $\mu = -2.5$, $\gamma = 0.5$ and $\chi = -0.2$. The profiles in the y-direction are slightly wider and the results are shown in dimensionless units.

Next, in figure 5, we display another PDE numerical simulation, where we can observe that the stability verified in figure 4 can be lost just by decreasing the strength of one of the linear OLs. In both the panels of figure 5 we have the same parameters considered in the upper panel of figure 4, except for the strength of the LOL in the z-direction, which is reduced to $\varepsilon_z = 2.5$ in the upper panel and further to $\varepsilon_z = 2.0$ in the lower panel. As shown, the stability still survives for $\varepsilon_z = 2.5$, but completely disappears in a very short-time interval when $\varepsilon_z = 2.0$ (in both the cases, we keep the strength in the x-direction fixed, $\varepsilon_x = 3.0$). Similar results (not shown) are also obtained for the repulsive case. In particular, for the case $\varepsilon_x = \varepsilon_z = 3.0$ is depicted in the lower right panel of figure 2 (see dotted curve), we found that by decreasing the strength of one of the LOL is enough to remove the observed stability. We have also confirmed for the more stable cases that by considering one direction unconstrained ($\varepsilon_z = 0$) no stable solution can be found with exact PDE simulations.

5. Conclusions

In this work we have investigated the existence of stable 3D solitons in cross-combined OLs, consisting of a LOL and a NOL along the x- and y-directions, respectively, with the z-direction either unconstrained (2D OL cross-combined case) or with another linear OL along this direction (3D OL cross-combined case). Two approaches are considered in our analysis: one analytical, by a variational approach, and the other by direct integration of the GP equation. The stability of the solutions was checked by using the VK criterion (in both the cases) and by the corresponding dynamical analysis, with direct numerical time evolution of the soliton profiles. Good agreement between the results obtained with VA and direct PDE calculations has been shown to exist in general. In particular, the agreement is improved for the 3D OL cross-combined case when the strengths of the LOLs are not too small.

In conclusion, for the main result of our analysis, we have shown that while in the 2D OL cross-combined case 3D solitons are always unstable, in the full 3D OL cross-combined case families of 3D solitons can exist and can be stable for both attractive and repulsive interactions. In perspective of potential applications, we should point out that besides providing an alternate way to create stable solitons in three dimensions, with cross-combined linear and nonlinear optical lattices (both in BEC and nonlinear optics), these results could be useful in practical applications, opening the possibility of managing stable 3D solitons through spatial modulations of the scattering length in one of the optical lattice directions.

Acknowledgments

FKA acknowledges support by the grant PIIF-GA-2009-236099 (NOMATOS) within the 7th European Community Framework Programme. AG, LT and HFLdL thank partial support from Fundação de Amparo à Pesquisa de São Paulo (FAPESP) and Conselho Nacional de Desenvolvimento Científico e Tecnológico (CNPq). MS acknowledges support from the Ministero dell' Istruzione, dell' Università e della Ricerca (MIUR) through a *Programma di Ricerca Scientifica di Rilevante Interesse Nazionale* (PRIN) initiative.

References

[1] Morsch O and Oberthaler M 2006 *Rev. Mod. Phys.* **78** 179
[2] Brazhnyi V A and Konotop V V 2004 *Mod. Phys. Lett.* B **18** 627
[3] Eiermann B, Anker Th, Albiez M, Taglieber M, Treutlein P, Marzlin K P and Oberthaler M K 2004 *Phys. Rev. Lett.* **92** 230401
[4] Kartashov Y V, Vysloukh V A and Torner L 2009 *Prog. Opt.* **52** 63
[5] Baizakov B B, Konotop V V and Salerno M 2002 *J. Phys. B: At. Mol. Opt. Phys.* **35** 5105
Ostrovskaya E A and Kivshar Yu S 2003 *Phys. Rev. Lett.* **90** 160407
[6] Baizakov B B, Malomed B A and Salerno M 2003 *Europhys. Lett.* **63** 642
[7] Baizakov B B, Malomed B A and Salerno M 2004 *Phys. Rev.* A **70** 053613
[8] Aközbek N and John S 1998 *Phys. Rev.* E **57** 2287
[9] Mihalache D, Mazilu D, Lederer F, Kartashov Y V, Crasovan L C and Torner L 2004 *Phys. Rev.* E **70** 055603
[10] Torner L and Kartashov Y V 2009 *Opt. Lett.* **34** 1129
[11] Ye F, Kartashov Y V, Hu B and Torner L 2009 *Opt. Express* **17** 11328
[12] Leblond H, Malomed B A and Mihalache D 2009 *Phys. Rev.* A **79** 033841
[13] Minardi S *et al* 2010 *Phys. Rev. Lett.* **105** 263901
[14] Abdullaev F Kh, Gammal A and Tomio L 2004 *J. Phys. B: At. Mol. Opt. Phys.* **37** 635
[15] Abdullaev F Kh, Kevrekidis P G and Salerno M 2010 *Phys. Rev. Lett.* **105** 113901
[16] Kartashov Y V, Malomed B A and Torner L 2011 *Rev. Mod. Phys.* **83** 247
[17] Cruz H A, Brazhnyi V A, Konotop V V and Salerno M 2009 *Physica* D **238** 1372
[18] Inouye S, Andrews M R, Stenger J, Miesner H J, Stamper-Kurn D M and Ketterle W 1998 *Nature* **392** 151
Stenger J, Inouye S, Andrews M R, Miesner H J, Stamper-Kurn D M and Ketterle W 1999 *Phys. Rev. Lett.* **82** 2422
Roberts J L, Claussen N R, Burke J P Jr, Greene C H, Cornell E A and Wieman C E 1998 *Phys. Rev. Lett.* **81** 5109
Cornish S L, Claussen N R, Roberts J L, Cornell E A and Wieman C E 2000 *Phys. Rev. Lett.* **85** 1795
Donley E A, Claussen N R, Cornish S L, Roberts J L, Cornell E A and Wieman C E 2001 *Nature* **412** 295
[19] Fedichev P O, Kagan Yu, Shlyapnikov G V and Walraven J T M 1996 *Phys. Rev. Lett.* **77** 2913
[20] Petrov D S and Shlyapnikov G V 2001 *Phys. Rev.* A **64** 012706
[21] Bludov Yu V and Konotop V V 2006 *Phys. Rev.* A **74** 043616
Abdullaev F Kh, Abdumalikov A A and Galimzyanov R M 2007 *Phys. Lett.* A **367** 149
Rodrigues A S *et al* 2008 *Phys. Rev.* A **78** 013611
[22] Cheng Y 2009 *J. Phys. B: At. Mol. Opt. Phys.* **42** 205005
Cheng Y and Adhikari S K 2011 *Phys. Rev.* A **83** 023620
[23] Yamazaki R, Taie S, Sugawa S and Takahashi Y 2010 *Phys. Rev. Lett.* **105** 050405
[24] Sakaguchi H and Malomed B A 2004 *J. Phys. B: At. Mol. Opt. Phys.* **37** 1443
Sakaguchi H and Malomed B A 2005 *Phys. Rev.* E **72** 046610
[25] Dong G and Hu B 2007 *Phys. Rev.* A **75** 013625
[26] Salerno M, Konotop V V and Bludov Yu V 2008 *Phys. Rev. Lett.* **101** 030405
[27] Bludov Yu V, Konotop V V and Salerno M 2009 *J. Phys. B: At. Mol. Opt. Phys.* **42** 105302
Bludov Yu V, Konotop V V and Salerno M 2009 *Europhys. Lett.* **8** 20004
[28] Bludov Yu V, Konotop V V and Salerno M 2011 *Europhys. Lett.* **93** 30003
[29] Abdullaev F Kh and Garnier J 2005 *Phys. Rev.* A **72** 061605
[30] Abdullaev F Kh, Galimzyanov R M, Brtka M and Tomio L 2009 *Phys. Rev.* E **79** 056220
[31] Fibich G, Sivan Y and Weinstein M I 2006 *Physica* D **217** 31
Sivan Y, Fibich G and Weinstein M I 2006 *Phys. Rev. Lett.* **97** 193902
[32] Hung N V, Zin P, Trippenbach M and Malomed B A 2010 *Phys. Rev.* E **82** 046602
[33] da Luz H L F, Abdullaev F Kh, Gammal A, Salerno M and Tomio L 2010 *Phys. Rev.* A **82** 043618
[34] Abdullaev F Kh, Gammal A, da Luz H L F and Tomio L 2007 *Phys. Rev.* A **76** 043611
[35] Abdullaev F Kh, Gammal A, Salerno M and Tomio L 2008 *Phys. Rev.* A **77** 023615
[36] Borovkova, O V Malomed B M and Kartashov Y V 2010 *Europhys. Lett.* **92** 64001
[37] Middelkamp S, Kevrekidis P G, Frantzeskakis D J, Carretero-González R and Schmelcher P 2010 *J. Phys. B: At. Mol. Opt. Phys.* **43** 155303
[38] Baizakov B B and Salerno M 2004 *Phys. Rev.* A **69** 013602
[39] Brtka M, Gammal A and Tomio L 2006 *Phys. Lett.* A **359** 339
[40] Vakhitov N G and Kolokolov A A 1973 *Radiophys. Quantum Electron.* **16** 783
[41] Sivan Y, Fibich G, Ilan B and Weinstein M I 2008 *Phys. Rev.* E **78** 046602
[42] Sakaguchi H and Malomed B A 2010 *Phys. Rev.* A **81** 013624
[43] Bohn J L and Julienne P S 1997 *Phys. Rev.* A **56** 1486